

High-pressure phase transition and metallization in $\text{Ar}(\text{H}_2)_2$

Yansun Yao (姚延荪) and Dennis D. Klug

Steacie Institute for Molecular Sciences, National Research Council of Canada, Ottawa, K1A 0R6, Canada

(Received 17 November 2010; published 24 January 2011)

The high-pressure phase transition and the metallization of $\text{Ar}(\text{H}_2)_2$ are investigated using first-principles methods. A phase transition from the experimentally observed MgZn_2 structure to a CeCu_2 -type structure is predicted near 66 GPa. This phase transition provides a possible explanation for the disappearance of the Raman active vibron mode in experiment between 55 and 70 GPa. The metallization of the CeCu_2 structure is promoted by the intermolecular interactions among H_2 molecules, but hindered by the modulation of Ar atoms. The competition between these two mechanisms implies that the pressure for metallization in $\text{Ar}(\text{H}_2)_2$ is higher than that suggested for pure hydrogen. This prediction is a result of an examination of a previous proposal that hydrogen could metallize at much lower pressure by mixing with Ar, and provides insight for future studies on metallization of hydrogen through the use of hydrogen-rich mixtures.

DOI: [10.1103/PhysRevB.83.020105](https://doi.org/10.1103/PhysRevB.83.020105)

PACS number(s): 64.70.kt, 61.50.Ks, 62.50.-p, 71.30.+h

One of the most fascinating pursuits in high-pressure science is the search for metallic hydrogen.¹ Sufficient compression can induce band overlap and/or molecular dissociation, which are considered as two alternative routes for hydrogen to reach the metallic state.^{2,3} The pressure required to produce metallic hydrogen, however, is predicted to be above 400 GPa, which is the limit of the current static experimental techniques.^{4,5} Recent studies indicate that mixtures of hydrogen with impurities may lower the pressure required for metallization.^{6–8} One experimental study,⁸ in particular, has shown that silane mixed with hydrogen may yield a much lower pressure for metallization. The potential importance for the use of hydrogen mixed with impurities has been summarized recently by Ashcroft.⁹ Impurities can enhance the intermolecular interactions in the system, by hybridizing the hydrogen bands and partially filling the unoccupied bands. Experimental evidence for this mechanism was suggested in the compression of an Ar + H_2 mixture.⁶ At 4.3 GPa, an Ar + H_2 mixture forms an ordered compound $\text{Ar}(\text{H}_2)_2$, identified as a *C14* Laves phase structure (isomorphous to MgZn_2). Based on Raman data, it has been suggested that H_2 in the MgZn_2 structure starts to dissociate near 175 GPa and becomes metallic.⁶ This experiment provided a possible approach for producing metallic hydrogen well within the current capability of experiments. Subsequent infrared (IR) measurement, however, did not confirm the Raman results, and showed that the molecular phase of $\text{Ar}(\text{H}_2)_2$ is stable to at least 220 GPa.¹⁰ Initial calculations suggested that the metallization of $\text{Ar}(\text{H}_2)_2$ occurs via a phase transition from the MgZn_2 to an *A1B₂*-type structure near 250 GPa.¹¹ However, other theoretical works predicted that the band gap of the *A1B₂* structure does not close until 420 GPa.¹² A recent theoretical study¹³ predicts the existence of a *C15* Laves phase structure (isomorphous to MgCu_2) at low temperature.

In view of the significant interest in examining mixtures as a possible route to hydrogen metallization, this study employs theoretical structural searches and property predictions since the difficulties that both experiments and theory encounter could be attributed to the lack of knowledge of the structures. The x-ray diffraction (XRD) study of $\text{Ar}(\text{H}_2)_2$, for example, was reported only at 6.2 GPa, and it was assumed that the MgZn_2 structure remains up to 175 GPa. The theoretically

predicted structures were previously guessed from other known *AB₂* models, e.g., Laves phases, but this now appears to be insufficient. In the present study, we extensively searched for high-pressure structures of $\text{Ar}(\text{H}_2)_2$ and predict a transition from the MgZn_2 structure to a CeCu_2 -type structure near 66 GPa. The H_2 molecules in the CeCu_2 structure locate in puckered layers and Ar atoms form chains to modulate the intermolecular interactions within the layers. Although certain impurities can facilitate band-gap closure, Ar atoms actually delay metallization of hydrogen in $\text{Ar}(\text{H}_2)_2$. The density-functional theory (DFT) calculation estimates that the band gap of $\text{Ar}(\text{H}_2)_2$ closes at a higher pressure than that estimated for pure hydrogen.

Candidate structure searches of $\text{Ar}(\text{H}_2)_2$ were performed at pressures between 50 and 200 GPa with the “random search” method¹⁴ with primitive cells containing 2 and 4 $\text{Ar}(\text{H}_2)_2$ units. Structural optimizations, charge densities, electronic band structures, and density of states (DOS) were calculated using the Vienna *ab initio* simulation (VASP) code¹⁵ and projector-augmented plane-wave (PAW) potentials.¹⁶ The Ar potential employed $3s^23p^6$ as valence state, with the Perdew-Burke-Ernzerhof (PBE) exchange-correlation functional¹⁷ and an energy cutoff of 910 eV. An $8 \times 8 \times 8$ and a $32 \times 32 \times 32$ *k*-point mesh¹⁸ were used in the total-energy and DOS calculations, respectively. Phonons, Raman, and IR intensities were calculated using the ABINIT program¹⁹ and Hartwigsen-Goedecker-Hutter (HGH) or Troullier-Martins pseudopotentials^{20,21} with an energy cutoff of 60 Ha, along with a $4 \times 4 \times 4$ *q*-point and a $10 \times 10 \times 10$ *k*-point mesh.

The calculated enthalpies of the most stable candidates are compared in Fig. 1(a) over the pressure range 0–300 GPa. Below 66 GPa, the MgCu_2 structure is marginally the most stable structure. The experimentally observed MgZn_2 structure has slightly higher enthalpy [< 0.008 eV/f.u.; 1 formula unit (f.u.) = 1 $\text{Ar}(\text{H}_2)_2$]. Near 66 GPa, a predicted CeCu_2 structure becomes the most stable, and its enthalpy is overwhelmingly lower than all other candidates. A calculation of the quasiharmonic vibrational free energy at 300 K and 155 GPa using the phonon DOS (Ref. 22) decreases the free-energy difference between the CeCu_2 and the MgCu_2 structures by only about 0.04 eV/f.u. and implies that the transition pressure increases by about 10 GPa. The *A1B₂* structure, although more stable

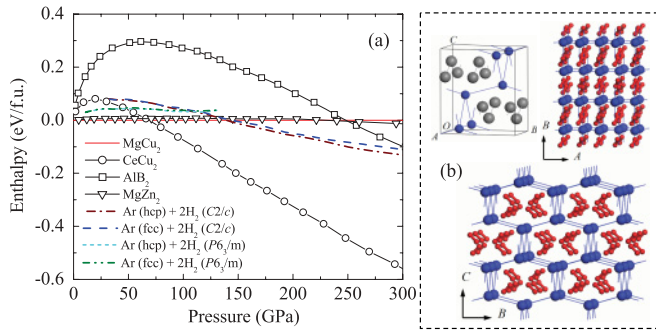


FIG. 1. (Color online) (a) Calculated enthalpies as functions of pressure for candidate $\text{Ar}(\text{H}_2)_2$ structures and decompositions ($\text{Ar} + 2\text{H}_2$) relative to that of the MgCu_2 structure. (b) CeCu_2 structure of $\text{Ar}(\text{H}_2)_2$. The basic CeCu_2 lattice is shown in upper left with Ar atoms represented by smaller balls and the H_2 molecules (as one entity) represented by bigger balls. The detailed H_2 orientation is shown in the upper right and bottom, with the H_2 molecules represented by dumbbells.

than the MgZn_2 structure near 250 GPa, has much higher enthalpy than the CeCu_2 structure. The possibility of decomposition in $\text{Ar}(\text{H}_2)_2$ is checked by comparing the enthalpy of $\text{Ar}(\text{H}_2)_2$ with that of $\text{Ar} + 2\text{H}_2$ [Fig. 1(a)]. The structures for pure hydrogen were the previously proposed phases,²³ $P6_3/m$ (<105 GPa) and $C2/c$ (>105 GPa). The structures used for Ar were the two co-existing phases in this pressure range, fcc and hcp.²⁴ Up to at least 300 GPa, the most stable phase of $\text{Ar}(\text{H}_2)_2$ always has lower enthalpy than $\text{Ar} + 2\text{H}_2$, indicating that decomposition is unlikely. Above 130 GPa, the CeCu_2 structure is essentially the only structure of $\text{Ar}(\text{H}_2)_2$ that does not decompose into $\text{Ar} + 2\text{H}_2$. Previous experiments also provided evidence for this predicted phase transition. The MgZn_2 structure of $\text{Ar}(\text{H}_2)_2$ was identified by an XRD study at 6.2 GPa, and has been suggested as a stable phase up to at least 50 GPa by a spectroscopic study.²⁵ However, the structure of $\text{Ar}(\text{H}_2)_2$ above 50 GPa is not known. In Raman measurements,⁶ the H_2 vibron mode of $\text{Ar}(\text{H}_2)_2$ is reported to disappear between 55 and 70 GPa, and was originally assumed to be due to changes in orientational ordering of H_2 . One may, however, expect that a more radical structural change to the CeCu_2 structure results in a lower sample Raman scattering quality or another intermediate structure.

The CeCu_2 structure is described by the orthorhombic space group $Imma$, with Ar occupying $4e$ sites and H_2 molecular centers of mass located at $8h$ sites [Fig. 1(b)]. The structural parameters for the CeCu_2 structure, for example, at 66 GPa, are $4e$: 0, 0.25, 0.0621; $8h$: 0, 0.0632, 0.6659, and $a = 3.19 \text{ \AA}$, $b = 5.29 \text{ \AA}$, $c = 5.89 \text{ \AA}$. The H_2 molecules rotate freely in $\text{Ar}(\text{H}_2)_2$ at low pressure,²⁵ and are therefore represented by their center-of-mass positions in the CeCu_2 structure. However, each H_2 molecule is represented by its two H atoms to calculate the lowest enthalpy configuration for the structures shown in Fig. 1(a). A full optimization of the CeCu_2 structure that includes the lowest enthalpy H_2 molecular orientation lowers the space group to $C2/c$. In the $C2/c$ space group, the molecular axes of all H_2 molecules are parallel to the crystal plane $(1\bar{1}0)$ of the orthorhombic unit cell, and the H_2 molecules on different planes alternatively tilt and yield angles with

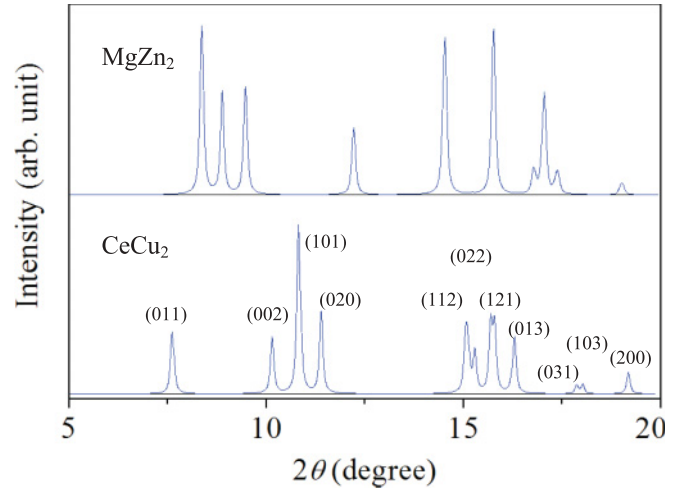


FIG. 2. (Color online) Calculated XRD patterns (x-ray wavelength = 0.5 \AA) for optimized MgZn_2 and CeCu_2 structures near 103 GPa.

respect to the $[110]$ direction by $\pm 38.8^\circ$. The intramolecular H-H distance is 0.727 \AA for all H_2 molecules. The calculated XRD pattern of the optimized CeCu_2 structure is presented in Fig. 2 with a full width at half maximum (FWHM) of $0.1 (2\theta)$ for the peak shape.²⁶ All Bragg peaks can be indexed with the CeCu_2 structure as marked, with the only slight distortion in the (121) peak resulting from a full optimization. The calculated XRD pattern of the MgZn_2 structure at a similar pressure (Fig. 2) illustrates the distinct difference between these two structures. The CeCu_2 structure might be considered as a low-symmetry variant of the hexagonal AlB_2 structure (space group $P6/mmm$). One can transform the orthorhombic unit cell to a hexagonal supercell by decreasing the cla ratio to 1.732, in order to then identify the xz plane as the xy plane of the hexagonal lattice. Simultaneously, one needs to slightly modify some of the internal coordinates to yield the $P6/mmm$ space group. By changing z to 0.0 while keeping x and y fixed, the $4e$ sites would convert to the $1a$ sites in the $P6/mmm$ space group. By changing y and z to 0.0 and 0.6666, respectively, while keeping x fixed, the $8h$ sites would convert to the $2d$ sites in the $P6/mmm$ space group. From this description, the CeCu_2 structure can be obtained from an AlB_2 structure by (1) straining the hexagonal Ar planes (yielding an orthorhombic unit cell) and shearing the neighboring planes ($1a$ sites become $4e$ sites), plus (2) straining the hexagonal H_2 plane and puckering the planes ($2d$ sites become $8h$ sites).

The calculated band gap of the CeCu_2 structure of $\text{Ar}(\text{H}_2)_2$ closes near 350 GPa [Fig. 3(a) and Ref. 22], which is higher than the originally suggested value of 175 GPa.⁶ For pure hydrogen, using the proposed $C2/c$ structure as a candidate, the calculated pressure for the band-gap closure is about 300 GPa [Fig. 3(a) and Ref. 22], even lower than that required for $\text{Ar}(\text{H}_2)_2$. Due to the deficiency of DFT associated with local-density or generalized-gradient approximations, the calculated band gaps are likely to be underestimated for both $\text{Ar}(\text{H}_2)_2$ and pure hydrogen. A previous study²⁷ shows that, for pure hydrogen, exact-exchange DFT leads to considerably (1–2 eV) larger energy gaps than the standard DFT values. If one adds 2 eV to the hydrogen band gaps and extrapolates

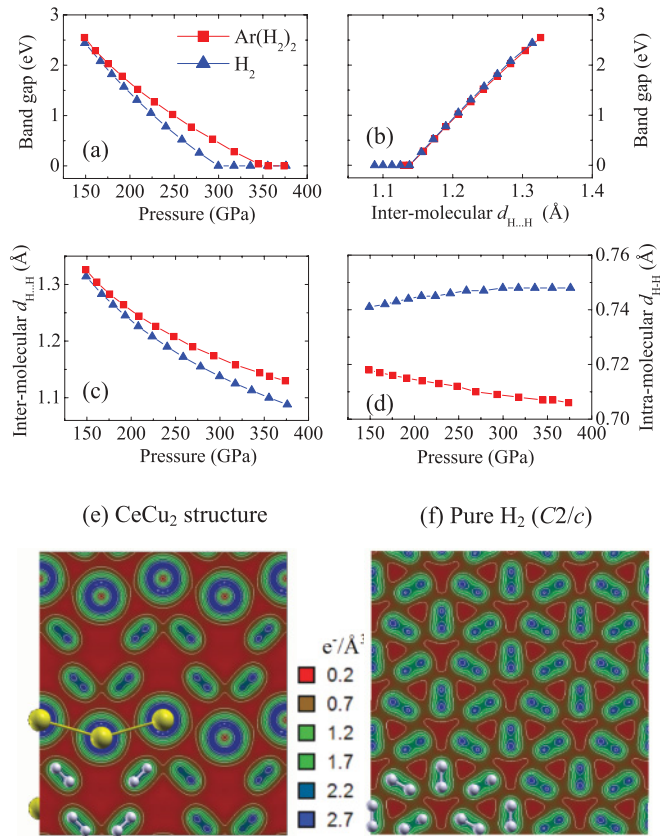


FIG. 3. (Color online) Calculated magnitudes of the band gap for $\text{Ar}(\text{H}_2)_2$ (CeCu₂ structure) and pure hydrogen (C2/c structure) (a) as functions of pressure, and (b) as functions of the nearest intermolecular H...H distance, $d_{\text{H}\dots\text{H}}$. Calculated (c) $d_{\text{H}\dots\text{H}}$ and (d) $d_{\text{H-H}}$ for $\text{Ar}(\text{H}_2)_2$ and pure hydrogen as functions of pressure. Calculated valence charge density for (e) $\text{Ar}(\text{H}_2)_2$ and (f) pure hydrogen at 300 GPa differentiated by a color scheme from red (light gray, low density, $0.2e^-/\text{\AA}^3$ or lower) to blue (dark grey, high density, $2.7e^-/\text{\AA}^3$ or higher). The Ar atoms and H_2 molecules are only shown in selected sites in (e) and (f).

the data, a band gap of C2/c hydrogen would close near 450 GPa. This agrees with the experiments for pure hydrogen that remains insulating up to at least 320 GPa.²⁸ In order for $\text{Ar}(\text{H}_2)_2$ to have the band-gap closure at a similar extrapolated pressure, a much smaller value of 0.8 eV should be added to the $\text{Ar}(\text{H}_2)_2$ band gaps. This analysis suggests that unless the DFT underestimates the band gap much more significantly for pure hydrogen than for $\text{Ar}(\text{H}_2)_2$, the speculation that hydrogen could metallize at much lower pressure by mixing with Ar is not predicted to occur.

The metallization of hydrogen is directly related to intermolecular interactions. With increasing pressure, the molecular orbitals of H_2 are delocalized and start to overlap. As intermolecular distances decrease, enhanced orbital overlap lowers energy levels of the intermolecular bonding states with respect to that of the antibonding states, and therefore increases the bandwidth and decreases the energy gap. A measure of the orbital overlaps is the nearest intermolecular H...H distance, $d_{\text{H}\dots\text{H}}$, and a shorter $d_{\text{H}\dots\text{H}}$ usually corresponds to larger orbital overlap. Notably, both $\text{Ar}(\text{H}_2)_2$ and pure hydrogen reach the

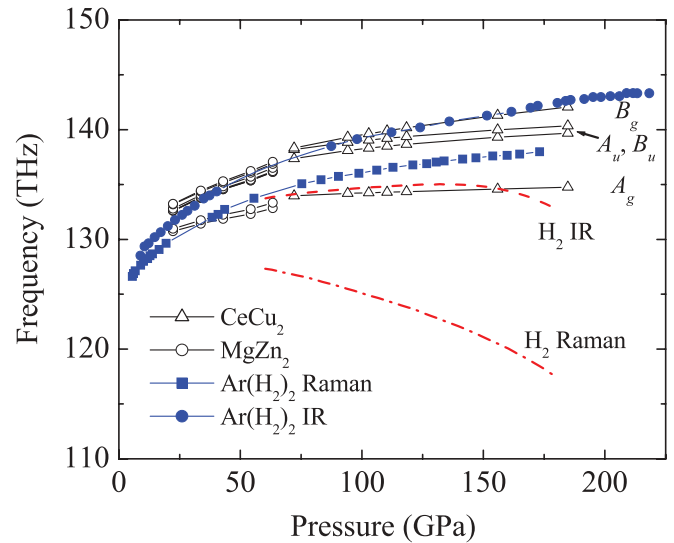


FIG. 4. (Color online) Calculated vibron frequencies for the MgZn_2 and CeCu_2 structures as functions of pressure, and compared with the experimental IR and Raman data for $\text{Ar}(\text{H}_2)_2$ and pure H_2 . The Raman data of $\text{Ar}(\text{H}_2)_2$ are from Ref. 6. The IR data of $\text{Ar}(\text{H}_2)_2$ below 50 GPa and above 87 GPa are from Refs. 25 and 10, respectively. The IR and Raman data for pure H_2 are from Refs. 29 and 30, and were collected at 295 K.

metallic state when their $d_{\text{H}\dots\text{H}}$ approaches the same value, i.e., 1.14\AA [Fig. 3(b)], but to reach this value, $\text{Ar}(\text{H}_2)_2$ needs greater compression [Fig. 3(c)]. The addition of Ar to H_2 when the H_2 is already fixed at the volume for metallization will therefore result in an increase of the pressure required for a metallic state. To analyze the orbital overlap, the valence charge density of the CeCu₂ structure calculated at 300 GPa is displayed on the (100) plane that features a puckered H_2 layer modulated by Ar chains [Fig. 3(e)]. For comparison, the calculated valence charge density of the C2/c hydrogen at the same pressure is also displayed on a H_2 layer [Fig. 3(f)]. Figure 3(e) shows that Ar interacts weakly with H_2 in $\text{Ar}(\text{H}_2)_2$, mainly due to the fully occupied Ar valence shells. Since Ar atoms occupy a large volume, the packing of H_2 in $\text{Ar}(\text{H}_2)_2$ is less dense when compared with pure hydrogen at the same pressure, as seen from the free space within the layers [Fig. 3(e)]. The Ar modulation therefore acts to separate H_2 molecules and prevent interactions among them. This is in contrast to the effects of other impurities that can strongly hybridize the H_2 orbitals and facilitate metallization.⁸ The orbital overlaps also affect the stability of H_2 molecules. For pure hydrogen, the H-H bonds begin to weaken above 40 GPa, as indicated by the decrease of Raman H_2 vibron frequencies with increasing pressure.²⁹ Using the intramolecular H-H distance, $d_{\text{H-H}}$, as a measure, the present calculation [Fig. 3(d)] shows no indication of bond weakening in $\text{Ar}(\text{H}_2)_2$ up to at least 375 GPa, and the H_2 molecules are well preserved in the metallic state of $\text{Ar}(\text{H}_2)_2$. This result agrees with the Raman data and shows that the metallic state of $\text{Ar}(\text{H}_2)_2$ is reached without molecular dissociation.⁶

The stability of the predicted CeCu₂ structure of $\text{Ar}(\text{H}_2)_2$ is established from phonon calculations. The absence of imaginary frequencies confirms stability of the CeCu₂ structure.²²

In Fig. 4, the vibron frequencies calculated for MgZn₂ and CeCu₂ structures are shown, along with the experimental IR and Raman data for Ar (H₂)₂ (Refs. 6, 10, and 25) and pure hydrogen.^{29,30} The highest and lowest vibron modes are calculated to be Raman active but the calculated intensity of the high-frequency B_g Raman mode is only about 3% of the low-frequency A_g vibron. The calculated absorption intensity of the A_u symmetry IR active mode is about 8% of that of the close in frequency B_u IR active mode. The calculated frequencies of the IR and Raman modes are lower than the experiment by 0.75% and 2.2% at 150 GPa, respectively. The frequencies of the CeCu₂ structures increase with pressure, consistent with experiment, and as described above, result from H-H bond strengthening [Fig. 3(d)]. The vibron frequencies from MgZn₂ and CeCu₂ structures also show a good continuity. The Raman vibron disappears in experiment between 55 and 70 GPa—it seems reasonable to relate this to a MgZn₂ → CeCu₂ transition. The IR data are absent in this pressure range and therefore do not provide further information. Nevertheless, the frequencies of the IR active modes for the CeCu₂ structure agree very well with the

available IR data. Considering that additional factors affect the vibron frequencies, e.g., rotational modes and quantum effects, the agreement between the experiment and the current calculations is reasonable.

In summary, we present a theoretical study of high-pressure phase transition and the metallization of Ar(H₂)₂. The calculations predict a phase transition from the known MgZn₂ structure to a CeCu₂-type structure near 66 GPa, which could explain the observed disappearance of the Raman active vibron mode in this pressure range. The competition between the overlapping H₂ orbitals, which enhance band expansion, and Ar modulation, which prevents the intermolecular interactions, yields a pressure for metallization in Ar(H₂)₂ even higher than that suggested for bulk hydrogen. The addition of Ar to bulk H₂ will delay the metallization of H₂. This study therefore provides a critical examination of the possibility of producing metallic hydrogen at much lower pressure by mixing with Ar. The results obtained by combining structure search methods and *ab initio* properties predictions for Ar(H₂)₂ in the present study will hopefully provide insight and guidance to future experiments that employ mixtures of hydrogen plus impurities.

-
- ¹N. W. Ashcroft, *Phys. Rev. Lett.* **21**, 1748 (1968).
²E. Wigner and H. B. Huntington, *J. Chem. Phys.* **3**, 764 (1935).
³T. W. Barbee, A. Garcia, M. L. Cohen, and J. L. Martins, *Phys. Rev. Lett.* **62**, 1150 (1989).
⁴B. Edwards and N. W. Ashcroft, *Nature (London)* **388**, 621 (1997).
⁵A. F. Goncharov *et al.*, *Proc. Natl. Acad. Sci. U.S.A.* **98**, 14234 (2001).
⁶P. Loubeyre, R. Letoullec, and J.-P. Pinceaux, *Phys. Rev. Lett.* **72**, 1360 (1994).
⁷N. W. Ashcroft, *Phys. Rev. Lett.* **92**, 187002 (2004).
⁸T. A. Strobel, M. Somayazulu, and R. J. Hemley, *Phys. Rev. Lett.* **103**, 065701 (2009).
⁹N. W. Ashcroft, *Physics* **2**, 65 (2009).
¹⁰R. J. Hemley, *Annu. Rev. Phys. Chem.* **51**, 763 (2000).
¹¹S. Bernard, P. Loubeyre, and G. Zérah, *Europhys. Lett.* **37**, 477 (1997).
¹²N. Matsumoto and H. Nagara, *J. Phys.: Condens. Matter* **19**, 365237 (2007).
¹³C. Cazorla and D. Errandonea, *Phys. Rev. B* **81**, 104108 (2010).
¹⁴C. J. Pickard and R. J. Needs, *Phys. Rev. Lett.* **97**, 045504 (2006).
¹⁵G. Kresse and J. Hafner, *Phys. Rev. B* **47**, 558 (1993).
¹⁶G. Kresse and D. Joubert, *Phys. Rev. B* **59**, 1758 (1999).
¹⁷J. P. Perdew, K. Burke, and M. Ernzerhof, *Phys. Rev. Lett.* **77**, 3865 (1996).
¹⁸H. J. Monkhorst and J. D. Pack, *Phys. Rev. B* **13**, 5188 (1976).
¹⁹X. Gonze *et al.*, *Comput. Mater. Sci.* **25**, 478 (2002).
²⁰M. Krack, *Theor. Chem. Acc.* **114**, 145 (2005).
²¹N. Troullier and J. L. Martins, *Phys. Rev. B* **43**, 1993 (1991).
²²See supplemental material at [<http://link.aps.org/supplemental/10.1103/PhysRevB.83.020105>] for electronic and phonon densities of states and band structures for CeCu₂ and MgCu₂ structures of Ar(H₂)₂; electronic band structures for the C2/c structure of hydrogen.
²³C. J. Pickard and R. J. Needs, *Nature Phys.* **3**, 473 (2007).
²⁴D. Errandonea, R. Boehler, S. Japel, M. Mezouar, and L. R. Benedetti, *Phys. Rev. B* **73**, 092106 (2006).
²⁵L. Ulivi, R. Bini, P. Loubeyre, R. LeToullec, and H. J. Jodl, *Phys. Rev. B* **60**, 6502 (1999).
²⁶C. F. Macrae *et al.*, *J. Appl. Crystallogr.* **39**, 453 (2006).
²⁷M. Städele and R. M. Martin, *Phys. Rev. Lett.* **84**, 6070 (2000).
²⁸P. Loubeyre, F. Occelli, and R. LeToullec, *Nature (London)* **416**, 613 (2002).
²⁹H. K. Mao and R. J. Hemley, *Rev. Mod. Phys.* **66**, 671 (1994).
³⁰M. Hanfland, R. J. Hemley, H. K. Mao, and G. P. Williams, *Phys. Rev. Lett.* **69**, 1129 (1992).